The Astrophysical Journal Letters, 928:L21 (7pp), 2022 April 1 https://doi.org/10.3847/2041-8213/ac6107

Markovian Features of the Solar Wind at Subproton Scales

Simone Benella[1], Mirko Stumpo[2,1], Giuseppe Consolini[1], Tommaso Alberti[1], Vincenzo Carbone[3], and Monica Laurenza[1]
[1] INAF-Istituto di Astrofisica e Planetologia Spaziali, I-00133 Roma, Italy; simone.benella@inaf.it
[2] Dip. Fisica, Università degli Studi di Roma Tor Vergata, I-00133 Roma, Italy
[3] Dipartimento di Fisica, Università della Calabria, Rende (CS), I-87036, Italy
Received 2022 January 21; revised 2022 March 3; accepted 2022 March 11; published 2022 April 5

Abstract

The interplanetary magnetic field carried out from the Sun by the solar wind displays fluctuations over a wide range of scales. While at large scales, say at frequencies lower than 0.1–1 Hz, fluctuations display the universal character of fully developed turbulence with a well-defined Kolmogorov-like inertial range, the physical and dynamical properties of the small-scale regime as well as their connection with the large-scale ones are still a debated topic. In this work we investigate the near-Sun magnetic field fluctuations at subproton scales by analyzing the Markov property of fluctuations and recovering basic information about the nature of the energy transfer across different scales. By evaluating the Kramers–Moyal coefficients we find that fluctuations in the subproton range are well described as a Markovian process with Probability Density Functions (PDFs) modeled via a Fokker–Planck (FP) equation. Furthermore, we show that the shape of the PDFs is globally scale-invariant and similar to the one recovered for the stationary solution of the FP equation at different scales. The relevance of our results on the Markovian character of subproton scale fluctuations is also discussed in connection with the occurrence of turbulence in this domain.

Unified Astronomy Thesaurus concepts: Solar wind (1534); Interplanetary turbulence (830); Magnetohydrodynamics (1964); Heliosphere (711); Interplanetary physics (827); Space plasmas (1544)

1. Introduction

The recently launched Parker Solar Probe (PSP) mission (Fox et al. 2016) has increased the interest in investigating the evolution of solar wind properties through the inner heliosphere. Several studies have been performed to investigate the near-Sun or pristine solar wind properties (Bale et al. 2019) and to characterize the radial evolution of magnetic field fluctuations at different heliocentric distances in terms of high-order statistics of increments (Alberti et al. 2020), spectral features (Chen et al. 2020), the entropic character of magnetic field fluctuations (Stumpo et al. 2021), and the emergence of large-scale rapid polarity reversals known as switchbacks (de Wit et al. 2020). PSP measurements allow not only to investigate the solar wind features at different heliocentric distances, but also to characterize the dynamics of its fluctuations over a wide range of scales, from the large scales up to the subproton regime. The inertial range properties, i.e., the behavior of magnetic field fluctuations between the integral scale L and the ion inertial length scale d_i, seem to be consistent with expectations from the magnetohydrodynamic turbulence picture of describing the solar wind fluctuations in a fluid-like approximation, whereas the behavior of fluctuations in the subproton regime, i.e., at scales smaller than d_i, still remains unclear and highly debated (Chhiber et al. 2021).

The characterization of physical processes operating across the inertial range and responsible for transferring energy toward smaller scales has been broadly investigated in terms of stochastic processes. This is a long-standing idea since pioneering works by Ruelle & Takens (1971) and Mandelbrot (1978). In the framework of hydrodynamic turbulence it has been shown that the statistics of longitudinal velocity increments can be described in terms of the Markov *process in scale* (Pedrizzetti & Novikov 1994; Friedrich & Peinke 1997; Davoudi & Tabar 1999; Renner et al. 2001a). Indeed, the main idea behind these works is to represent the statistics of the longitudinal velocity increments as a stochastic process evolving across the length or timescales, instead of the common evolution in space or in time. A similar approach aiming to study the Markovian properties of the solar wind magnetic field fluctuations in the inertial range has been used by Strumik & Macek (2008a, 2008b) in the framework of space plasma turbulence. They showed that the turbulent cascade in the solar wind satisfies the Markov condition, suggesting the presence of a local energy transfer mechanism between subsequent scales which therefore does not depend on large-scale structures or the driving mechanisms of solar wind turbulence. However, this kind of study for the subproton regime is still missing. One of the striking features of this regime is the existence of a scale-invariant nature suggesting a filamentary structure of the dissipation field (Alberti et al. 2021). It has been also interpreted as the existence of a scale-invariant topology of current sheets between ion and electron inertial scales (Chhiber et al. 2021), leading the system toward a restored symmetry of the statistics of fluctuations (Dubrulle 2019). Nevertheless, there is no general consensus on the physical mechanisms explaining these small-scale features, which are generally highlighted through spacecraft measurements and are not observed through numerical simulations (Papini et al. 2019, 2021).

The properties of the magnetic field fluctuation statistics, expressed in terms of the scaling of power spectrum and structure functions, display a universal character in the inertial range of plasma turbulence. Conversely, in the subproton range a deep understanding of these statistical properties is still missing. In this paper we investigate the Markovian character

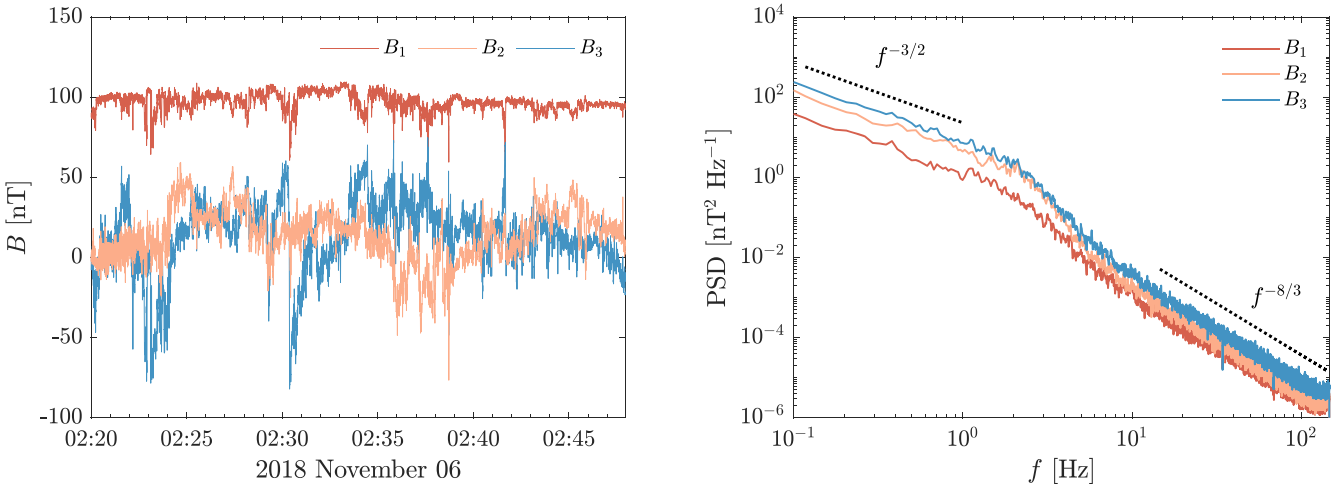

Figure 1. Left panel: the time series of the minimum (B_1), intermediate (B_2), and maximum (B_3) variance components of the magnetic field. Right panel: the corresponding PSDs. Dashed lines refer to power-law trends characterized by spectral slopes $-3/2$ at low frequencies and $-8/3$ at high frequencies, respectively.

of the magnetic field fluctuations at subproton scales by using high-resolution measurements gathered by PSP in the near-Sun solar wind for the first time. We provide a parameterization of the Kramers–Moyal (KM) coefficients associated with the magnetic field fluctuations as a function of the timescale. We show that the timescale evolution of the probability density functions (PDFs) is governed by the Fokker–Planck (FP) equation. As already shown in previous works, the shape of the experimental PDFs exhibits a global scale invariance. In this work we show that these pdfs can be successfully approximated by considering the stationary solution of the corresponding FP equation, contrary to what is generally observed in the inertial range of fully developed turbulence.

2. Data Description and Methods

2.1. Data

We investigate the statistics of the magnetic field increments at subproton scales in the pristine solar wind by using measurements gathered by the FIELDS suite on board PSP (Bale et al. 2016). Specifically, we focus on a 28 minute interval on 2018 November 6 from 02:20:00 UT to 02:48:00 UT, when PSP was located at about 0.17 au from the Sun. We use data from the SCaM data product in the spacecraft reference frame, which merges measurements from the fluxgate (FGM) and the search-coil (SCM) magnetometers, enabling observations from DC up to 1 MHz with an optimal signal-to-noise ratio (Bowen et al. 2020). Here, we consider data with a sampling of 293 samples s^{-1}, corresponding to $\sim$0.0034 s time resolution.

Since the spacecraft reference frame has no particular significance for our results, we rotate the magnetic field components in the minimum variance reference system, where B_1, B_2, and B_3 are the minimum, intermediate, and maximum variance components, respectively. The minimum variance component mainly resides along the radial direction while intermediate and maximum variance components are representative of fluctuations along the transverse directions with respect to the mean field.

Figure 1 shows the time series of the magnetic field components (left panel) along with the corresponding Power Spectral Densities (PSDs, right panel). As usually observed the PSDs show two different spectral behaviors $f^{-\beta}$: at low frequencies (i.e., $f \lesssim 1$ Hz) $\beta \in [3/2,\ 5/3]$ (in agreement with recent findings, Chen et al. 2020; Alberti et al. 2021; Chhiber et al. 2021), while in the subproton domain (i.e., $f \gtrsim 10$ Hz) $\beta \in [7/3,\ 8/3]$ (Chhiber et al. 2021). Moreover, a transition region is also observed between the two different dynamical regimes, with exponents showing a transition from inertial to subproton range behavior.

2.2. Methods

A fundamental quantity in the analysis of solar wind turbulence is represented by the magnetic field increment (fluctuation) across a time separation scale τ, defined as

$$b_{i,\tau} \doteq B_i(t+\tau) - B_i(t), \quad i = 1,\ 2,\ 3. \tag{1}$$

These increments represent a stochastic process in τ, thus it is relevant to investigate their Markovian character. Given a stochastic process $x(t,\ \tau)$, the main quantity in defining a Markov process is the transition probability, i.e., the probability of observing the state x_1 at the scale τ_1 given the states x_2 at the scale τ_2 until x_n at the scale τ_n, with $\tau_1 < \tau_2 < \ldots < \tau_n$. The process is Markovian if the n-point transition probability satisfies the condition

$$p(x_1,\ \tau_1|x_2,\ \tau_2;\ \ldots\ ;x_n,\ \tau_n) = p(x_1,\ \tau_1|x_2,\ \tau_2), \tag{2}$$

and then the knowledge of the initial distribution $p(x_n,\ \tau_n)$ and the two-points transition probabilities allows a complete knowledge of n-point probability distribution.

An important relation arising from the Markov condition is the Chapman–Kolmogorov (CK) equation expressing the transition probability of observing x_1 at the scale τ_1 given x_3 at the scale τ_3 by integrating on a variable x_2 at an arbitrary intermediate scale $\tau_1 < \tau_2 < \tau_3$ (Risken 1996, p. 28; Renner et al. 2001a), i.e.,

$$p(x_1,\ \tau_1|x_3,\ \tau_3) = \int_{-\infty}^{+\infty} p(x_1,\ \tau_1|x_2,\ \tau_2)p(x_2,\ \tau_2|x_3,\ \tau_3)dx_2. \tag{3}$$

The differential form of the CK equation is called the *master equation* and reads as

$$-\frac{\partial}{\partial\tau}p(x,\ \tau|x',\ \tau') = \mathcal{L}_{KM}(x,\ \tau)p(x,\ \tau|x',\ \tau'). \tag{4}$$

Equation (4) expresses the time evolution of the transition probability in terms of the KM expansion and the minus sign on the left-hand side of Equation (4) is due to the direction of the time evolution toward smaller scales (Renner et al. 2001a). Here, the operator $\mathcal{L}_{KM}(x)$ is the KM operator,

$$\mathcal{L}_{KM}(x, \tau) = \sum_{k=1}^{\infty}\left(-\frac{\partial}{\partial x}\right)^{k} D^{(k)}(x, \tau), \tag{5}$$

where the functions $D^{(k)}(x, \tau)$ are the KM coefficients.

For a generic stochastic Markov process, all the terms in the KM expansion are different from zero. However, according to the Pawula's theorem, if the fourth-order coefficient $D^{(4)}(x, \tau)$ is equal to zero, all the coefficients of order $k \geqslant 3$ vanish and the KM expansion stops at the second order. In that case, the KM expansion reduces to the FP equation (Risken 1996)

$$-\frac{\partial}{\partial \tau}p(x, \tau|x', \tau') = \left[-\frac{\partial}{\partial x}D^{(1)}(x, \tau) + \frac{\partial^2}{\partial x^2}D^{(2)}(x, \tau)\right]p(x, \tau|x', \tau'). \tag{6}$$

The first-order KM coefficient $D^{(1)}(x, \tau)$ represents the *drift* function, accounting for the deterministic evolution of the stochastic process x, whereas the second-order KM coefficient $D^{(2)}(x, \tau)$ constitutes the *diffusion* term, which modulates the amplitude of the delta-correlated Gaussian noise, $\Gamma(\tau)$, of the corresponding Langevin equation

$$-\frac{\partial x}{\partial \tau} = D^{(1)}(x, \tau) + \sqrt{D^{(2)}(x, \tau)}\,\Gamma(\tau). \tag{7}$$

From a practical point of view, the KM coefficients are not directly accessible from data, but rather they can be evaluated by using the conditional moments. According to Renner et al. (2001a, 2001b), the k^{th}-order conditional moment is defined as

$$M^{(k)}_{\Delta\tau}(x, \tau) = \int_{-\infty}^{+\infty}(x\,' - x)^k p(x', \tau - \Delta\tau|x, \tau)dx'. \tag{8}$$

The corresponding k^{th}-order KM coefficient is defined by taking the limit

$$D^{(k)}(x, \tau) = \frac{1}{k!}\lim_{\Delta\tau\to 0}\frac{1}{\Delta\tau}M^{(k)}_{\Delta\tau}(x, \tau). \tag{9}$$

Whereas conditional moments defined in (8) can be computed from the experimental observations, the definition (9) cannot be applied exactly. In fact, the best estimate of the k^{th}-order KM coefficient considered in the analysis is given by

$$D^{(k)}_{\tau_s}(x, \tau) = \frac{1}{k!\tau_s}M^{(k)}_{\tau_s}(x, \tau), \tag{10}$$

where τ_s indicates the time resolution of the time series.

Here, we applied the above analysis to the small-scale increments of the magnetic field at the subproton scales, starting from the verification of the CK Equation (3), and successively evaluating the KM coefficients up to the fourth order.

3. Results

The first step of our analysis consists in searching for the Markovian nature of the statistics of increments $b_{i,\tau}$. Although the analysis is performed in the temporal domain, it is possible to assume that we are exploring spatial scales via Taylor's hypothesis, i.e., $r = \tau V_{SW}$ where V_{SW} is the solar wind velocity. This hypothesis has been shown to be valid in the selected time interval being solar wind supersonic and super-Alfvénic (e.g., Chhiber et al. 2021; Perez et al. 2021). In the following we show the results for the minimum, intermediate, and maximum variance directions. One way to test the Markov condition on the statistics of increments is to prove that Equation (3) is satisfied for the stochastic process defined by the increments $b_{i,\tau}$ at different timescales. In the following, we set the small timescale $\tau_1 = 0.01$ s and we show results for three different values of the timescale separation $\Delta\tau = 0.0034$, 0.01, and 0.5 s. The intermediate timescale is then evaluated as $\tau_2 = \tau_1 + \Delta\tau$, while the large timescale as $\tau_3 = \tau_1 + 2\Delta\tau$. The statistics of increments at these scales allow us to evaluate and compare both members of Equation (3). We refer to the left-hand side of Equation (3) as the empirical conditional probability, p_E, and to the right-hand side as the CK conditional probability p_{CK}. The results of the CK test are shown in Figure 2. Figures 2(a), 2(d), and 2(g) display a good agreement between p_E (red lines) and p_{CK} (blue lines) for $\Delta\tau = 0.0034$ s, suggesting that the process is Markovian at this scale. By increasing the separation to $\Delta\tau = 0.01$ s the Markov condition is still fulfilled in the whole subproton range, Figures 2(b), 2(e), and 2(h). However, by increasing the separation to $\Delta\tau = 0.5$ s, such to fall at the end of the inertial regime, the CK equation appears still valid, although neither p_E nor p_{CK} depends on the large scale increments b_{i,τ_3}, Figures 2(c), 2(f), and 2(i). Summarizing, for the considered data sample the scale-to-scale process defined by $b_{i,\tau}$ is in general markovian across the whole subproton domain and the fluctuation amplitudes in the subproton domain seem to be statistically independent from those observed in the inertial range, i.e., $p(b_{i,\tau_1}, \tau_1|b_{i,\tau_3}, \tau_3) = p(b_{i,\tau_1}, \tau_1)$. We emphasize that the same results have been obtained for all the values of τ_1 within the subproton range (not shown).

Previous studies showed that the Pawula theorem holds across the inertial range of turbulence. This implies that the evolution of the PDFs of field increments in the inertial domain is governed by Equation (6). This result has been accurately validated in the case of hydrodynamic and solar wind turbulence (see Renner et al. 2001a; Strumik & Macek 2008b; Peinke et al. 2019, and references therein), while there is no evidence yet at subproton scales. Thus, we first assess its validity by computing the finite-timescale KM coefficients of the process $b_{i,\tau}$ at the sampling time τ_s, Equation (10). Figure 3 shows that the fourth-order KM coefficient is close to zero for both components suggesting that the Pawula theorem is also valid in the subproton domain. Hence, the evolution of the PDFs of magnetic field increments is governed by the FP equation. Furthermore, it is evident that the first-order coefficient is a linear function of $b_{i,\tau}$, whereas the second-order coefficient shows a quadratic trend. Thus, we can introduce the following parameterization for $D^{(1)}_{\tau_s}$ and $D^{(2)}_{\tau_s}$ as

$$D^{(1)}_{\tau_s}(b_i, \tau) = -\gamma_i(\tau)b_i, \tag{11}$$

$$D^{(2)}_{\tau_s}(b_i, \tau) = \alpha_i(\tau) + \beta_i(\tau)b_i^2, \tag{12}$$

such that we can study the dependence of the parameters $\gamma_i(\tau)$, $\alpha_i(\tau)$, and $\beta_i(\tau)$ upon the timescale τ. All parameters exhibit a power-law dependence on the timescale τ, i.e.,

$$\{\alpha_i(\tau), \beta_i(\tau), \gamma_i(\tau)\} = A_0\tau^{\mu}, \tag{13}$$

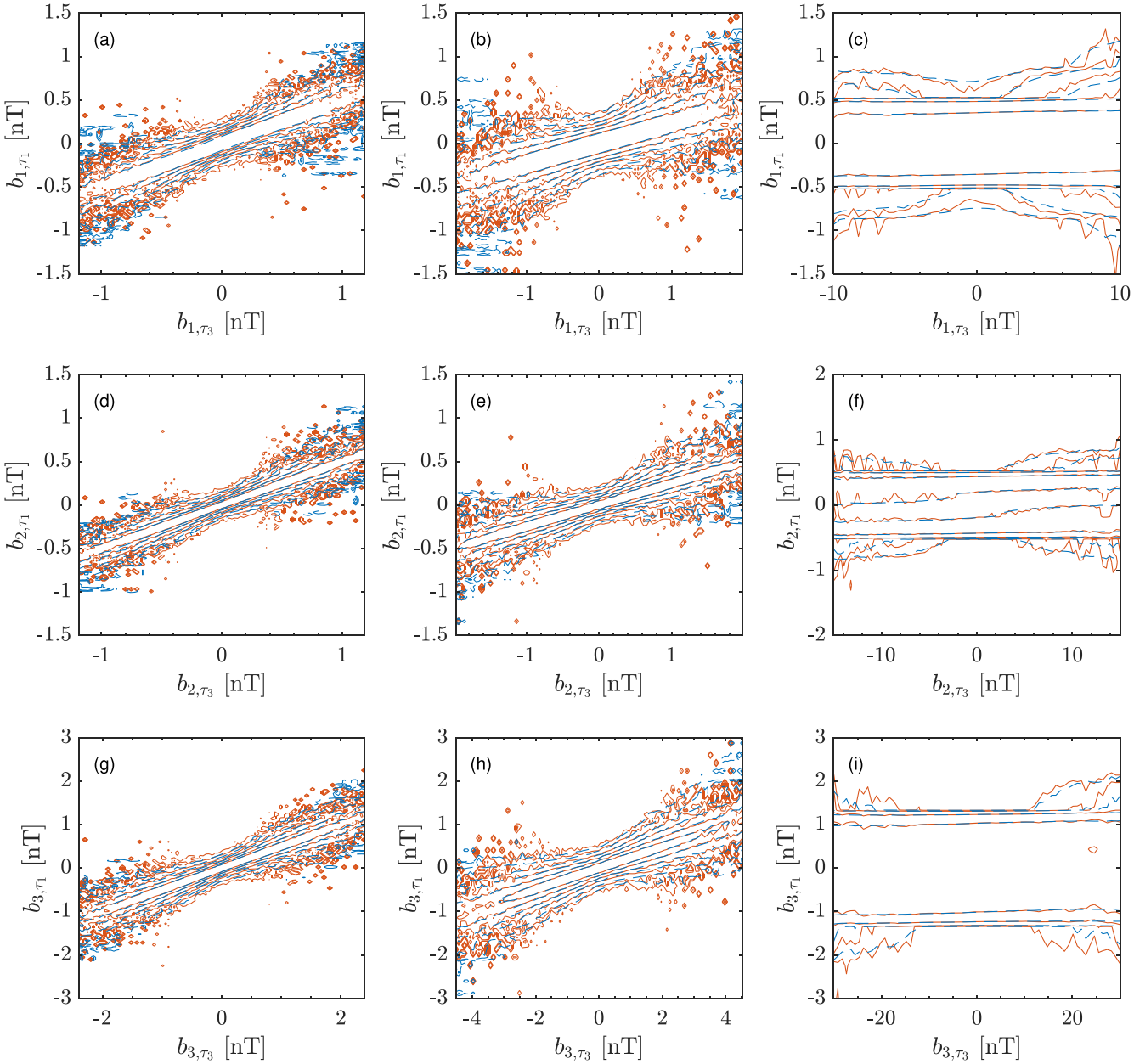

Figure 2. Comparison between observed (red curves) and reconstructed (blue curves) conditional probabilities at different timescales for minimum (upper panels), intermediate (middle panels), and maximum (lower panels) variance directions. The timescale differences $2\,\Delta\tau = \tau_3 - \tau_1$ for the CK test are 0.0068 s (panels a, d, and g), 0.02 s (panels b, e, and h), and 1.0 s (panels c, f, and i).

and the values of A_0 and μ are listed in Table 1 for the three magnetic field components.

As a further step, we perform a consistency check by computing the evolution of the PDFs of the magnetic field increments from large toward small scales in the subproton domain. We start from $p(b_{i,\tau_0})$ at $\tau_0 = 0.051$ s as an initial condition, and then we compute the numerical solution of the FP equation by assuming a Gaussian short-time propagator (Renner et al. 2001b). Figures 4(a), 4(b), and 4(c) show the comparison between the empirical PDFs and the corresponding FP numerical solutions. The excellent agreement between the empirical PDFs and the theoretical predictions proves that the FP equation with the KM coefficients (11) and (12) accurately describes the evolution of PDFs in the subproton domain.

Furthermore, by rescaling the PDFs at the different scales according to the following transformations, (e.g., see Figures 4(d), 4(e), and 4(f), circles),

$$b_{i,\tau} \longrightarrow x_i \equiv \frac{b_{i,\tau}}{\sigma_{b_{i,\tau}}}, \tag{14}$$

$$p(b_{i,\tau}) \longrightarrow p(x_i) \equiv \sigma_{b_{i,\tau}} p(b_{i,\tau}) \tag{15}$$

where $\sigma_{b_{i,\tau}}$ is the standard deviation of $b_{i,\tau}$, we obtained a PDF collapsing in the subproton range (Kiyani et al. 2009; Osman et al. 2015; Chhiber et al. 2021). The PDF collapsing defines a *master curve* for the shape of the PDFs. Thus, we attempt a comparison between the experimental PDFs of the rescaled increments and the corresponding stationary solutions of the FP equation. We evaluate the stationary distribution $p_{\rm ST}(x_i)$ by solving the timescale independent FP equation (Risken 1996),

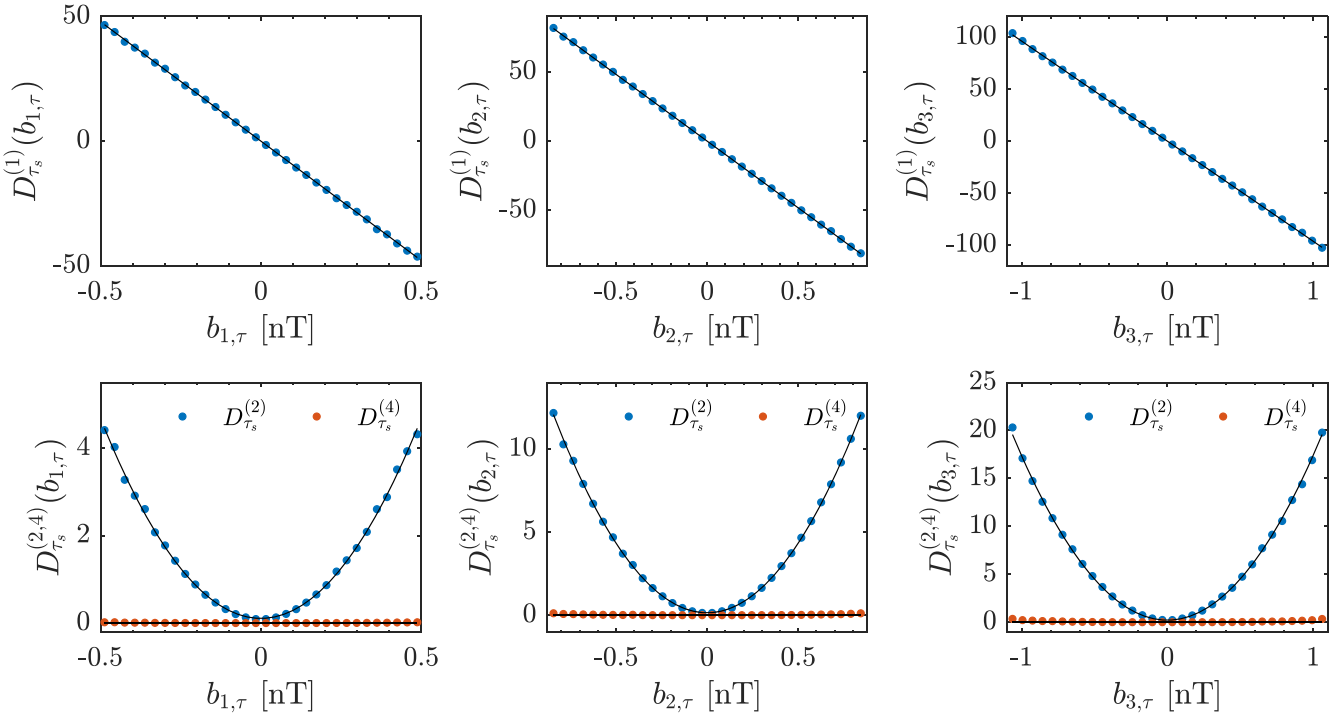

Figure 3. First, second, and fourth-order finite-size KM coefficients for $b_{1,\tau}$ (left), $b_{2,\tau}$ (center), and $b_{3,\tau}$ (right) at scale $\tau = 0.01$ s. Solid lines represent the $D^{(1,2)}_{\tau_s}(b_{i,\tau})$ best fit and $D^{(4)}_{\tau_s}(b_{i,\tau}) = 0$.

Table 1
Fitted Coefficients A_0 and μ of Equation (13)

	$b_{1,\tau}$		$b_{2,\tau}$		$b_{3,\tau}$	
	A_0	μ	A_0	μ	A_0	μ
α	0.7 ± 0.2	0.36 ± 0.08	1.6 ± 0.3	0.47 ± 0.06	5.3 ± 1.7	0.61 ± 0.08
β	0.003 ± 0.001	-1.87 ± 0.01	0.002 ± 0.001	-1.96 ± 0.01	0.002 ± 0.001	-1.98 ± 0.01
γ	0.87 ± 0.03	-1.01 ± 0.01	0.90 ± 0.02	-1.01 ± 0.01	0.89 ± 0.02	-1.02 ± 0.01

i.e.,

$$\frac{\partial}{\partial x_i}[D^{(2)}(x_i)p_{\rm ST}(x_i)] = \frac{D^{(1)}(x_i)}{D^{(2)}(x_i)}D^{(2)}(x_i)p_{\rm ST}(x_i). \quad (16)$$

By introducing the set of KM coefficients $D^{(1)}(x_i) = -\gamma_i x_i$ and $D^{(2)}(x_i) = \alpha_i + \beta_i x_i^2$ in (16), where α_i, β_i, and γ_i are now constants, the stationary solution reads

$$p_{\rm ST}(x_i) = N_0(\alpha_i + \beta_i x_i^2)^{-\frac{\gamma_i}{2\beta_i}-1}, \quad (17)$$

where N_0 is the normalization factor. We may note how the obtained function is a Kappa distribution (Milovanov & Zelenyi 2000; Leubner & Vörös 2005), which can be written also in the standard form,

$$p_{\rm ST}(x_i) = N'_0\left[1 + \frac{1}{\kappa}\frac{x_i^2}{x_0^2}\right]^{-\kappa}, \quad (18)$$

where $\kappa = 1 + \gamma_i/2\beta_i$, $x_0^2 = 2\alpha_i/(\gamma_i + 2\beta_i)$ and $N'_0 = N_0\alpha_i^{-\kappa}$.

Whereas the inertial range is characterized by strongly intermittent magnetic field fluctuations reflecting in a well-known modification of the PDF shape moving from the scale of the forcing toward the dissipation scale, the subproton range statistics exhibit a global scale invariance that manifests in the existence of a *shape-invariant* master curve. The comparison between the empirical PDFs of the normalized variables x_i and the stationary PDFs are reported in Figures 4(d), 4(e), and 4(f). The values of the parameters of Equation (18) obtained by fitting the distributions are $N_0' = 0.58$, $x_0 = 0.75$, and $\kappa = 2.0$ for x_1, $N_0' = 0.54$, $x_0 = 0.83$, and $\kappa = 2.1$ for x_2, and $N_0' = 0.53$, $x_0 = 0.85$, and $\kappa = 2.1$ for x_3. We stress that in this framework the FP equation describes the evolution of PDFs across timescales instead of time, and thus the concept of stationarity has to be intended as invariance of the rescaled magnetic field increment PDFs for any timescale in the subproton range. The agreement between the observed PDFs and Equation (18) is remarkably good. However, we point out that this stationary distribution has to be considered as a valid approximation of the core of the empirical PDFs in a restricted range of variability of x_i (e.g., within $\pm 5\sigma$ as shown in the bottom panel of Figure 4). Indeed, in this figure it is evident that the tails of the distributions display a slight departure from the stationary solution, especially for x_2 and x_3, and for increasing values of x_i the tails of the empirical PDFs decrease more rapidly than the tails of the Kappa distribution.

4. Discussion and Conclusions

In this work we have investigated the Markovian character of the magnetic field increments (fluctuations) at subproton scales

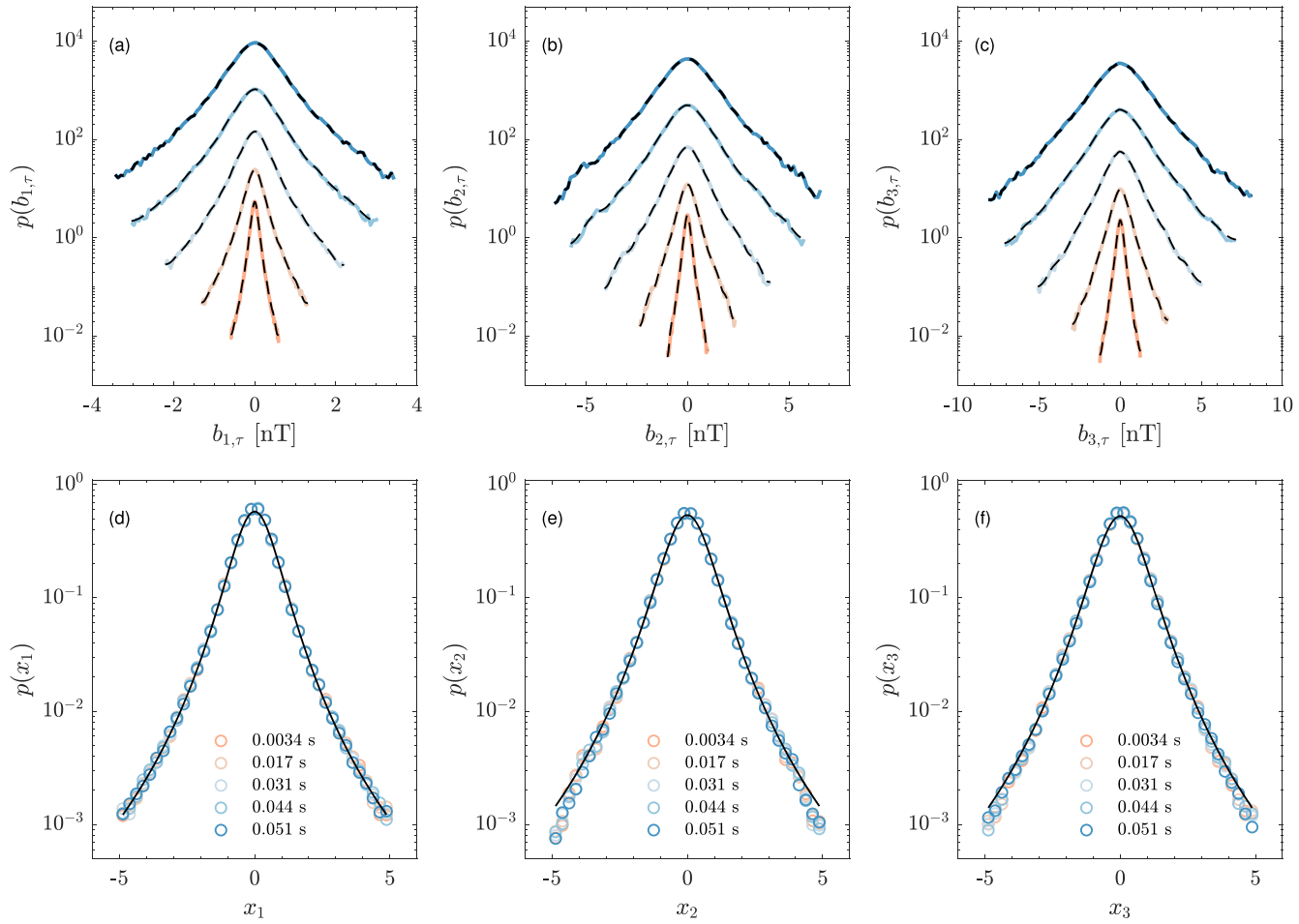

Figure 4. Comparison of the empirical PDFs $p(b_{i,\tau})$ obtained from the PSP data at different scales (colored lines) with the numerical solutions (dashed lines), panels (a), (b), and (c). All the curves are shifted in the vertical direction for clarity of presentation and correspond to the following timescales, from top to bottom: 0.051, 0.044, 0.031, 0.017, and 0.0068 s. Panels (d), (e), and (f) show the data collapsing of empirical PDFs, circles, along with the best fit of the stationary solution (18), solid lines.

in turbulent near-Sun solar wind. The results clearly evidenced that at these scale, as already observed in the inertial range (Strumik & Macek 2008a, 2008b), the statistics of the magnetic field fluctuations are Markovian and the dynamics along the different scales can be described in terms of a FP equation. Since universality based on some turbulent-like approach to fluctuations is lost at small scales, different approaches based on some basic concepts of nonequilibrium statistical mechanics, such as the one presented here, could successfully reveal some universal characteristics of the underlying processes which generate fluctuations at these scales (Carbone et al. 2022).

On the physical side, we obtain that the energy transfer has a local character. Although this feature is also present in the inertial range of the solar wind, our analysis shows that no statistical correspondence is found between magnetic field fluctuations observed in inertial and subproton regimes. The observed statistical independence does not mean that there is no energy flux from the inertial domain toward the subproton scales but suggests that the mechanisms at the origin of the fluctuations observed in the two regimes are different. Moreover, in various recent and past works it was found that the scaling of structure functions of magnetic field increments at subproton scales suggests the occurrence of *global scale invariance*, i.e., lack of intermittency. This is clearly supported by the existence of a scale-invariant shape of the PDFs of magnetic field increments, whose shape is well approximated by the stationary solution of the FP equations. Furthermore, we show that by using the common linear and quadratic parameterizations for the first and second KM coefficients, respectively, the scale-invariant distribution coming from the stationary FP equation is the Kappa distribution (18). Since κ depends on γ_i and β_i, the KM coefficients can be related to the supposed nonextensive character of fluctuations. Indeed, considering Equation (18) and reminding its relation between κ and the nonextensivity parameter q of Tsallis' entropy, i.e., $\kappa = 1/(1-q)$, from the relation $q = \gamma_i/(2\beta_i + \gamma_i)$ we obtain $q \sim 0.5$ for the three magnetic field components. These values do not differ significantly from those measured by Leubner & Vörös (2005) in the low end of the inertial range of solar wind magnetic field fluctuations.

As a last point, we would like to discuss the physical consequences of the observed global scale invariance. As already mentioned above, the emergence of global scale invariance at subproton scales means that we do not observe intermittency in this regime. This can be linked to the fact that the statistics of the magnetic field increments can be successfully approximated by the stationary solution of the FP equation with respect to the

timescale variable τ. This is equivalent to assuming that the probability flux is constant across the scales, i.e., $\partial p/\partial \tau \rightarrow 0$ and $p \rightarrow p_{\rm ST}$. From a speculative point of view, the absence of intermittency could indicate that the scaling properties in this regime could be more realistically related to the formation of a self-similar current structure, which is an expected dissipative structure. In other words, the cascade mechanism in the inertial range ends with the formation of a topological structure that is a complex fractal representing, de facto, the dissipative pattern. Thus, the observed scale invariance could be the counterpart of the fractal topology of the current structure. Clearly, this is a speculative point of view, which, however, could represent the starting point for successive investigation and analysis. An alternative scenario could be the occurrence of wave turbulence in the subproton range such that the cascade mechanism may be better described in terms of an energy transfer flow toward the electron scales where heating and dissipation might occur.

In conclusion, here we have provided strong evidence for the Markovian character of the small-scale magnetic field fluctuations at subproton scales along with other strong evidence of the global scale invariant character of these fluctuations on the considered data sample. These results represent a possible indication for finding universal features in the magnetic field fluctuation statistics at subproton scales in terms of Markov processes. Further work is necessary in order to unveil similar statistical properties in different samples of high-frequency interplanetary magnetic field observations.

The data used in this study are available at the NASA Space Physics Data Facility (SPDF), https://spdf.gsfc.nasa.gov/index.html. The authors acknowledge the contributions of the FIELDS team to the Parker Solar Probe mission. This work is funded by the Italian MIUR-PRIN grant 2017APKP7T on "Circumterrestrial Environment: Impact of Sun-Earth Interaction." M.S. acknowledges the PhD course in Astronomy, Astrophysics and Space Science of the University of Rome "Sapienza," University of Rome "Tor Vergata" and Italian National Institute for Astrophysics (INAF), Italy.

ORCID iDs

Simone Benella https://orcid.org/0000-0002-7102-5032
Mirko Stumpo https://orcid.org/0000-0002-6303-5329
Giuseppe Consolini https://orcid.org/0000-0002-3403-647X
Tommaso Alberti https://orcid.org/0000-0001-6096-0220
Vincenzo Carbone https://orcid.org/0000-0002-3182-6679
Monica Laurenza https://orcid.org/0000-0001-5481-4534

References

Alberti, T., Faranda, D., Donner, R. V., et al. 2021, ApJL, 914, L6
Alberti, T., Laurenza, M., Consolini, G., et al. 2020, ApJ, 902, 84
Bale, S., Goetz, K., Harvey, P., et al. 2016, SSRv, 204, 49
Bale, S., Badman, S., Bonnell, J., et al. 2019, Natur, 576, 237
Bowen, T. A., Bale, S. D., Bonnell, J. W., et al. 2020, JGRA, 125, e2020JA027813
Carbone, V., Telloni, D., Lepreti, F., & Vecchio, A. 2022, ApJL, 924, L26
Chen, C., Bale, S., Bonnell, J., et al. 2020, ApJS, 246, 53
Chhiber, R., Matthaeus, W. H., Bowen, T. A., & Bale, S. D. 2021, ApJL, 911, L7
Davoudi, J., & Tabar, M. R. R. 1999, PhRvL, 82, 1680
de Wit, T. D., Krasnoselskikh, V. V., Bale, S. D., et al. 2020, ApJS, 246, 39
Dubrulle, B. 2019, JFM, 867, P1
Fox, N., Velli, M., Bale, S., et al. 2016, SSRv, 204, 7
Friedrich, R., & Peinke, J. 1997, PhyD, 102, 147
Kiyani, K. H., Chapman, S. C., Khotyaintsev, Y. V., Dunlop, M. W., & Sahraoui, F. 2009, PhRvL, 103, 075006
Leubner, M., & Vörös, Z. 2005, ApJ, 618, 547
Mandelbrot, B. B. 1978, AnIPS, 2, 225
Milovanov, A., & Zelenyi, L. 2000, NPGeo, 7, 211
Osman, K. T., Kiyani, K. H., Matthaeus, W. H., et al. 2015, ApJL, 815, L24
Papini, E., Cicone, A., Franci, L., et al. 2021, ApJL, 917, L12
Papini, E., Franci, L., Landi, S., et al. 2019, ApJ, 870, 52
Pedrizzetti, G., & Novikov, E. A. 1994, JFM, 280, 69
Peinke, J., Tabar, M. R., & Wächter, M. 2019, ARCMP, 10, 107
Perez, J. C., Bourouaine, S., Chen, C. H., & Raouafi, N. E. 2021, A&A, 650, A22
Renner, C., Peinke, J., & Friedrich, R. 2001a, JFM, 433, 383
Renner, C., Peinke, J., & Friedrich, R. 2001b, PhyA, 298, 499
Risken, H. 1996, Fokker-planck equation (Berlin: Springer), 63
Ruelle, D., & Takens, F. 1971, CMaPh, 23, 343
Strumik, M., & Macek, W. 2008a, NPGeo, 15, 607
Strumik, M., & Macek, W. M. 2008b, PhRvE, 78, 026414
Stumpo, M., Quattrociocchi, V., Benella, S., Alberti, T., & Consolini, G. 2021, Atmos, 12, 321